

# Molecular Structure and Conformation of Chloronitromethane as Determined by Gas-Phase Electron Diffraction and Theoretical Calculations

Quang Shen,<sup>\*,†</sup> Jeffrey W. Brown,<sup>†</sup> John A. Malona,<sup>†</sup> John C. Cochran,<sup>†</sup> and Alan D. Richardson<sup>‡</sup>

Department of Chemistry, 13 Oak Drive, Colgate University, Hamilton, New York 13346, and Department of Chemistry, Oregon State University, Corvallis, Oregon 97336.

Received: February 21, 2006; In Final Form: April 17, 2006

The molecular structure of chloronitromethane was studied in the gas phase at a nozzle-tip temperature of 373 K. The experimental data were interpreted using a dynamic model where the molecules are undergoing torsional motion governed by a potential function:  $V = V_2/2x(1 - \cos 2\tau) + V_4/2x(1 - \cos 4\tau)$  with  $V_2 = 0.81(30)$  and  $V_4 = 0.12(40)$  kcal/mol ( $\tau$  is the dihedral angle between the C–Cl and N–O bond). The conformer with a zero degree dihedral angle is the most stable conformer. Comparison with results from HF/MP2/B3LYP 6-311G(d,p) calculations were made. The important geometrical parameter values (for the eclipsed form) obtained from least-squares refinements are the following:  $r(\text{C–H}) = 1.061(18)\text{\AA}$ ,  $r(\text{C–N}) = 1.509(5)\text{\AA}$ ,  $r(\text{N–O}) = 1.223(1)\text{\AA}$ ,  $r(\text{C–Cl}) = 1.742(2)\text{\AA}$ ,  $\angle\text{ClCN} = 115.2(7)^\circ$ ,  $\angle\text{O}_4\text{NC} = 118.9(10)^\circ$ ,  $\angle\text{O}_5\text{NC} = 114.9(16)^\circ$ , and  $\angle\text{ClCH} = 115(4)^\circ$ .

## Introduction

The torsional potential function of nitromethane has a sixfold barrier as a result of the presence of the methyl (threefold) and nitro (twofold) groups. The torsional potential function has the following form (where  $\tau$  is the dihedral angle between the C–H and N–O bonds):

$$V = V_6/2x(1 - \cos 6\tau) \quad (1)$$

This potential function gave minima at  $60^\circ$  intervals starting at  $0^\circ$ , and the barrier at  $\tau = 30^\circ$  was 6.03 cal/mol.<sup>1</sup> When one of the protons is replaced, the sixfold symmetry is reduced to either a twofold symmetry or a combination of a four- and twofold terms as described by the following equation:

$$V = V_2/2x(1 - \cos 2\tau) + V_4/2x(1 - \cos 4\tau) \quad (2)$$

The twofold symmetry would give minima at 0 and  $180^\circ$ , whereas the function with two- and fourfold terms could have minima at 0,  $90^\circ$ , and  $180^\circ$  with different energies at 0 and  $90^\circ$  (see Figure 1). We are interested in understanding the torsional potential about the C–N bond of nitromethane, investigating the effect of substitutions on the barrier height, the minima of the torsional potential function, the molecular structure, and in general, the correlations between the potential function and geometry.

A good candidate for the proposed investigation by gas-phase electron diffraction is chloronitromethane. Infrared and Raman spectra of liquid chloronitromethane and their deuterated analogues have been recorded, and the complete assignments of all of the fundamentals have been made.<sup>2</sup> In this study, the molecule was assumed to have  $C_s$  symmetry with the  $\text{NO}_2$  plane perpendicular to the C–Cl bond (perpendicular form). An electron diffraction study<sup>3</sup> on the title compound has been reported. Two models, (1) free rotation and (2) a twofold

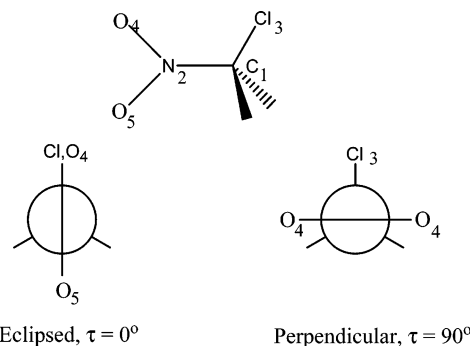


**Figure 1.** Atom numbering and the eclipsed and perpendicular forms for chloronitromethane ( $\tau = \text{O}_4\text{–N–C–Cl}$  dihedral angle).

rotational potential function (with the C–Cl/N–O dihedral angle of  $90^\circ$  as minimum) about the C–N bond, were used to fit the data. Careful examination of the published intensity and radial distribution curves, however, showed that neither one of these models gave a satisfactory agreement with the data. We therefore initiated an electron diffraction and theoretical investigation on this compound and are reporting the results here.

## Experimental Section

A sample of chloronitromethane was synthesized by adding sodium hydroxide (20% aq) dropwise to neat nitromethane at  $-5^\circ\text{C}$ . The resulting sodium methylnitronate was filtered and washed with liquid nitrogen to prevent decomposition. Once filtered, the sodium salt was suspended in anhydrous ethyl ether at  $-5^\circ\text{C}$  and chlorine gas was bubbled in for approximately 10 min. The resulting solution was decanted and the solvent evaporated, yielding a mixture of starting material, dichloronitromethane, and chloronitromethane. The desired product was obtained via distillation, bp  $102.5\text{--}104^\circ\text{C}$ .  $^1\text{H}$  and  $^{13}\text{C}$  NMR spectra were recorded in  $\text{CDCl}_3$  with a Bruker 400 MHz spectrometer.  $^1\text{H}$  NMR 5.70 ppm (s),  $^{13}\text{C}$  NMR 74.92 ppm (s).

Electron diffraction data were collected using the OSU apparatus at a nozzle-tip temperature of 373 K for the long

\* Corresponding author. E-mail: mshen@mail.colgate.edu.

<sup>†</sup> Colgate University.

<sup>‡</sup> Oregon State University.

**TABLE 1: Optimized Geometrical Parameters from HF/MP2/DFT 6-311G(d,p) Calculations<sup>a</sup>**

	HF		MP2		B3LYP	
	eclipsed	perpendicular	eclipsed	perpendicular	eclipsed	perpendicular
$r(\text{C}-\text{H})$	1.075	1.0738	1.0872	1.0864	1.0857	1.0845
$r(\text{N}-\text{O}_4)$	1.174	1.1823N	1.220	1.2276	1.2081	1.2173
$r(\text{N}-\text{O}_5)$	1.187	1.1823	1.2266	1.2276	1.2199	1.2174
$r(\text{C}-\text{N})$	1.4985	1.4912	1.5186	1.5008	1.5323	1.5193
$r(\text{C}-\text{Cl})$	1.7469	1.7601	1.7441	1.7575	1.7658	1.7800
$\angle\text{ClCN}$	113.97	109.53	113.47	109.63	113.85	109.91
$\angle\text{O}_4\text{NC}$	120.42	116.58	120.22	116.53	120.23	116.49
$\angle\text{O}_5\text{NC}$	112.75	116.58	112.57	116.53	112.41	116.49
$\angle\text{ONO}$	126.83	126.83	127.21	126.92	127.36	127.02
$\angle\text{HCN}$	105.5	107.28	105.28	106.97	105.45	107.16
$\angle\text{HCCl}$	110.35	109.36	110.75	109.69	110.27	109.19
$\tau\text{ClCN}_4$	0.11	89.98	0.086	89.44	0.075	89.86

<sup>a</sup> Distances in angstroms and angles in degrees.

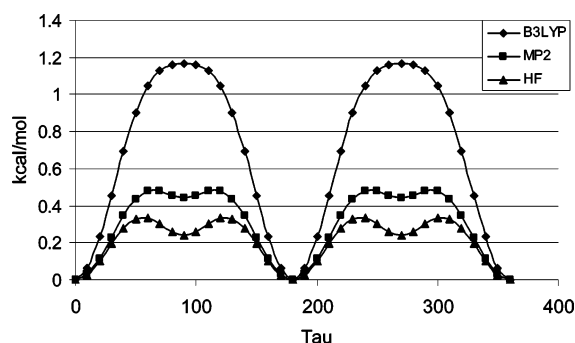


**Figure 2.** Torsional potential functions about the C–N bond obtained from ab initio calculations ( $\tau = \text{O}_4\text{--N--C--Cl}$  dihedral angle).

(746.15 mm) and 370 K for the middle (299.46 mm) camera distances, respectively. The voltage was maintained in the range of 60 keV. Beam currents in the range of 0.53–0.75  $\mu\text{A}$  and exposure times of 45–75 s for the long and 2–4 min for the middle camera plates were used. Four long camera and four mid-camera plates were selected for data analysis. Data reduction was carried out in the usual manner.<sup>4</sup> The intensity data were interpolated at integral units of  $q[=(40/\lambda) \sin(\theta/2)]$ , where  $2\theta$  is the scattering angle]. The intensity data were analyzed using a least-squares procedure outlined by Gundersen and Hedberg<sup>5</sup> using elastic scattering and phase factors calculated by Ross, Fink, and Hilderbrandt.<sup>6</sup>

### Calculations

Theoretical calculations were carried out at the HF, MP2, and B3LYP levels using 6-311G(d,p) and 6-311G++ basis sets available in Gaussian 98.<sup>7</sup> The geometrical parameters for the optimized eclipsed and perpendicular forms (Figure 1) from 6-311G(d,p) are summarized in Table 1. The C–N torsional potential function was obtained from complete optimization of the geometry with the Cl–C–N–O<sub>4</sub> dihedral angle held fixed at 10° increments. The torsional potential functions obtained are shown in Figure 2. The B3LYP, HF, and MP2 potentials were fitted to eq 2, and the  $V_2/V_4$  values obtained are: 1.17/0.22, 0.45/0.16, and 0.458/0.167 kcal/mol, respectively.

When 6-311G++ basis sets were used, all three levels of calculations gave potential functions of the form

$$V = V_2/2x(1 + \cos 2\tau) + V_4/2x(1 + \cos 4\tau) \quad (3)$$

with the minimum at the perpendicular form ( $\tau = 90^\circ$ ) instead of the eclipsed form as in the former calculations. The values for  $V_2/V_4$  are 0.17/–0.009, 0.89/–0.012, and 1.34/0.039 kcal/mol, and the barrier heights at eclipsed are 0.16, 0.90, and 1.5 kcal/

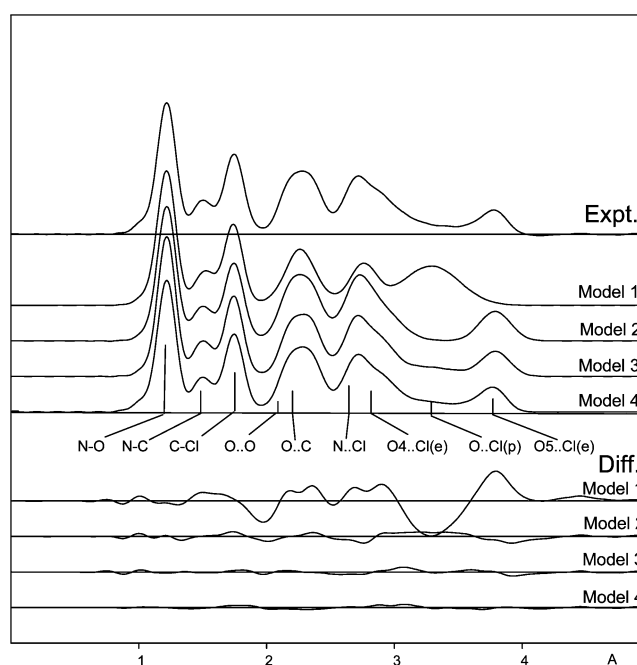


**Figure 3.** Radial distribution curves correspond to different theoretical models. Corresponding difference curves (experimental – theoretical) are shown under each group. The y axis represents the probability distribution of interatomic distances.

mol for DFT, HF, and MP2 calculations, respectively. The minimum is sensitive to the chosen basis sets, 6-311G(d,p) or 6-311G++. The former gave the eclipsed form, whereas the perpendicular form was predicted by the latter.

Frequency calculations (HF/6-311G(d,p)) were carried out for both the eclipsed and perpendicular forms, and the force fields from these calculations were used to obtain amplitudes of vibrations using ASYM40.<sup>8</sup>

**Electron Diffraction Analysis.** The molecular structure of chloronitromethane is defined by the following set of parameters:  $r(\text{C}-\text{H})$ ,  $r(\text{N}-\text{O})$ ,  $r(\text{C}-\text{N})$ ,  $r(\text{C}-\text{Cl})$ ,  $\angle\text{ClCN}$ ,  $\angle\text{ONC}$ ,  $\angle\text{O}_4\text{NC}$  and  $\angle\text{O}_5\text{NC}$ . The model of the perpendicular ( $\tau = 90^\circ$ ) form was tested first (model 1), and the errors in the nonbonded distances clearly showed that the data were not consistent with this model (Figure 3).

A model with the N–O bond eclipsing the C–Cl bond ( $\tau = 0^\circ$ ) was introduced. In this model (model 2), the following parameters are no longer identical:  $r(\text{N}-\text{O}_4)$  and  $r(\text{N}-\text{O}_5)$ ,  $\angle\text{O}_4\text{NC}$  and  $\angle\text{O}_5\text{NC}$ . MP2 calculations showed that  $r(\text{N}-\text{O}_4)$  is shorter than  $r(\text{C}-\text{O}_5)$  by 0.006 Å and  $\angle\text{O}_4\text{NC}$  is 7.6° larger than  $\angle\text{O}_5\text{NC}$ . These major structural differences were included

in the model. The radial distribution curve for this model is shown in Figure 3.

A two-conformer model (model 3) was tested. In this model, all of the structural differences between the eclipsed and perpendicular forms obtained from the MP2 calculations (see Table 1) were introduced in the model (i.e.,  $r(\text{C}-\text{Cl})$ ,  $r(\text{C}-\text{N})$ ,  $\angle\text{ClCN}$ ,  $\angle\text{O}_4\text{NC}$ , and  $\angle\text{O}_5\text{NC}$ ). Amplitude of vibration differences between the conformers (for example,  $l_{\text{O}_4\cdots\text{Cl}}$  and  $l_{\text{O}_5\cdots\text{Cl}}$ ) were also introduced. The best result from this model gave a composition of 70(8)% eclipsed and 30(8)% perpendicular forms and an  $R$  factor value of 7.4%. The corresponding radial distribution is shown in Figure 3.

Calculations suggested potential functions with two- and fourfold terms. The barrier obtained from HF, MP2, and B3LYP calculations are 0.30, 0.50, and 1.2 kcal/mol, respectively. A dynamic model (model 4) was introduced. In this model, restricted torsion motion about the C–N bond governed by eqs 2 (model 4a) and 3 (model 4b) were assumed. Equations 2 and 3 were potential functions obtained using 6-311G(d,p) and 6-311++G basis sets, respectively. The populations of the 10 conformers (in the range  $\tau = 0$  to  $90^\circ$  at  $10^\circ$  increments) were weighted using Boltzmann distribution.

Theoretical calculations showed that several geometrical parameters ( $r(\text{C}-\text{Cl})$ ,  $r(\text{C}-\text{N})$ ,  $\angle\text{ClCN}$ ,  $\angle\text{O}_4\text{NC}$ , and  $\angle\text{O}_5\text{NC}$ ) are sensitive to the dihedral angle,  $\tau$ . These variations are included in the 10 conformers in the following fashion. MP2 optimized values for these five parameters as a function of  $\tau$  (within the range of  $0^\circ$  to  $90^\circ$ ) were fitted and the following functions were obtained:

$$r(\text{C}-\text{Cl}) = r(\text{C}-\text{Cl})_{45} - 0.007x \cos 2\tau$$

$$r(\text{C}-\text{N}) = r(\text{C}-\text{N})_{45} + 0.010x \cos 2\tau$$

$$\angle\text{ClCN} = (\angle\text{ClCN})_{45} + 1.899x \cos 2\tau$$

$$\angle\text{O}_4\text{NC} = (\angle\text{O}_4\text{NC})_{90} + \Delta_1 x \cos \tau$$

$$\angle\text{O}_5\text{NC} = (\angle\text{O}_5\text{NC})_{90} - \Delta_1 x \cos \tau$$

where  $r(\text{C}-\text{Cl})_{45}$ ,  $r(\text{C}-\text{N})_{45}$ ,  $(\angle\text{ClCN})_{45}$ ,  $(\angle\text{O}_4\text{NC})_{90}$ , and  $(\angle\text{O}_5\text{NC})_{90}$  are the corresponding parameter values at the specified torsion angles ( $\tau = 45^\circ$ , and at  $90^\circ$  respectively) and these parameters were refined during the least-squares procedures. The numerical values are held constant as suggested by the calculated differences. The value for  $\Delta_1$  ( $\angle\text{O}_4\text{NC} - \angle\text{O}_5\text{NC}$ ) has a value of  $4^\circ$  initially and was later refined. There is only a slight difference between  $r(\text{N}-\text{O}_4)$  and  $r(\text{N}-\text{O}_5)$  of 0.006 Å at the eclipsed extreme; therefore, a single N–O bond was assumed in these dynamic models.

The amplitudes of vibration were calculated excluding the low-frequency torsional contribution. The  $\text{Cl}\cdots\text{O}_4$  and  $\text{Cl}\cdots\text{O}_5$  amplitudes of vibration were found to be sensitive to  $\tau$ , and the following functions were applied during the refinements:

$$l(\text{O}_4\cdots\text{Cl}) = l(\text{O}_4\cdots\text{Cl})_{90} + \Delta_2 x \sin(\tau)$$

$$l(\text{O}_5\cdots\text{Cl}) = l(\text{O}_5\cdots\text{Cl})_{90} - \Delta_3 x \sin(\tau)$$

where  $l(\text{O}_4\cdots\text{Cl})_{90}$  and  $l(\text{O}_5\cdots\text{Cl})_{90}$  are the corresponding  $\text{O}\cdots\text{Cl}$  amplitudes at the perpendicular form and the  $\Delta$  values are the calculated  $l_{ij}$  difference between 0 and  $90^\circ$  forms.

In model 4a, both  $V_2$  and  $V_4$  are refined values of 0.81(30) and 0.12(40) kcal/mol, respectively, with an  $R$  factor of 6.1%. Table 2 summarized the geometrical parameter values obtained

TABLE 2: Least-Squares Results for Chloronitromethane<sup>a</sup>

parameters		parameters	
$r(\text{C}-\text{H})$	1.061(18)	$\angle\text{ClCN}$	115.2(7)/111.4 <sup>b</sup>
$r(\text{N}-\text{O}_4)$	1.223(1)	$\angle\text{O}_4\text{NC}$	118.9(10)/116.9 <sup>b</sup>
$r(\text{C}-\text{N})$	1.509(5)/1.491 <sup>b</sup>	$\angle\text{O}_5\text{NC}$	114.9(11)/116.9 <sup>b</sup>
$r(\text{C}-\text{Cl})$	1.742(2)/1.756 <sup>b</sup>	$\angle\text{ClCH}$	115(4)
$V_2$	0.81(30)	$\angle\text{HCN}$	105.5(fixed)
$V_4$	0.12(40)		
$R^c$	6.2%		
$l_{\text{C}-\text{H}}$	0.0757/0.0757 <sup>d</sup>	$l_{\text{N}\cdots\text{Cl}}$	0.0725/0.071(6)
$l_{\text{N}-\text{O}}$	0.0382/0.041(1)	$l_{\text{O}\cdots\text{C}}$	0.0657/0.070(9)
$l_{\text{C}-\text{N}}$	0.0569/0.057(4)	$l_{\text{O}_4\cdots\text{Cl}}$	0.0837/0.084(15)
$l_{\text{C}-\text{Cl}}$	0.0513/0.049(2)	$l_{\text{O}_5\cdots\text{Cl}}$	0.067/0.067
$l_{\text{O}\cdots\text{O}}$	0.0479/0.052(5)		

<sup>a</sup> Distances in angstroms, angles in degrees, and energies in kcal/mol. <sup>b</sup> The values for the eclipsed/perpendicular forms that are different.

<sup>c</sup>  $R = \sum([I_{\text{ob}} - I_{\text{theo}}]^2 / I_{\text{obs}}^2)^{1/2}$ . <sup>d</sup> Calculated value/refined values followed by least-squares error limits.

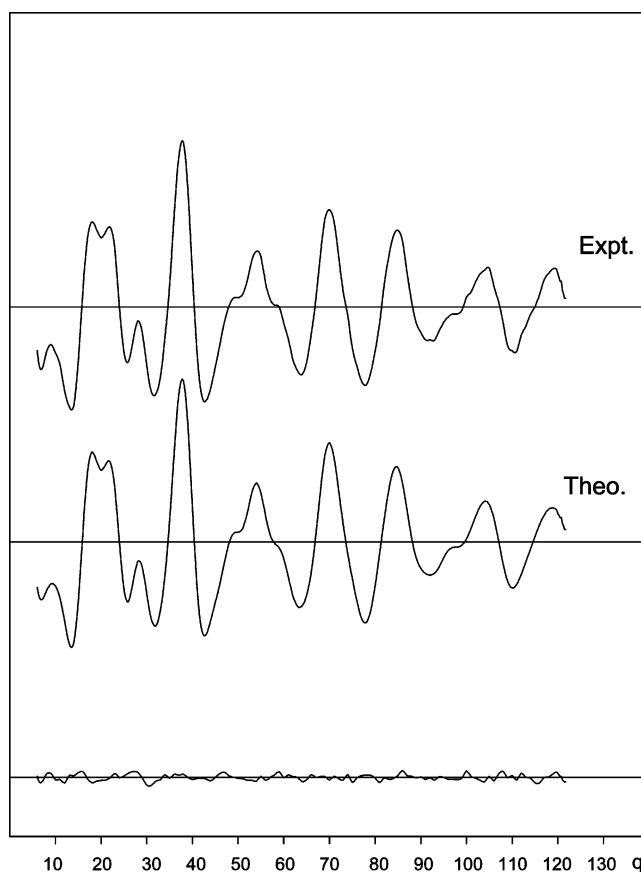
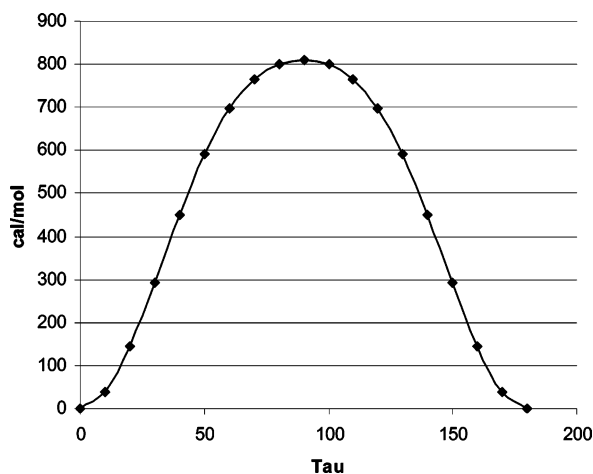


Figure 4. Intensity vs  $q$  curves correspond to model 4a ( $q = (40/\lambda) \sin(\theta/2)$ , where  $2\theta$  is the scattering angle; in units of  $\text{\AA}^{-1}$ ).

from least-squares refinements. The radial distribution, intensity, and torsional potential function curves are shown in Figures 3–5, respectively. Model 4b repeatedly converged to give negative  $V_2$  and  $V_4$  values yielding a potential function with the eclipsed form being more stable than the perpendicular form. The converged model 4b essentially gave conformation populations provided by eq 2.

## Discussion

The radial distribution curves obtained for models 1–4a were summarized in Figure 3. It is clear from models 1 and 2, and confirmed by model 3, that the majority of gaseous sample existed in eclipsed ( $\tau = 0.0^\circ$ ) form, which has  $\text{O}_4\cdots\text{Cl}$  and  $\text{O}_5\cdots\text{Cl}$  distances at 2.8 and 3.8 Å, respectively. For the perpen-



**Figure 5.** Experimental potential function about the C–N bond obtained from least-squares analysis.

dicular form, the corresponding distances are equal and have a value of 3.2 Å. The potential function obtained from model 4a is shown in Figure 5. This function is very similar to the one obtained from B3LYP 6-311G(d,p) calculations except for the barrier height at  $\tau = 90^\circ$ . Taking into account of the large experimental uncertainties in the  $V_2$  and  $V_4$  values, the agreement is very acceptable. Results from models 4a and b clearly show that the potential function from calculations using 6-311G(d,p) basis sets, eq 2, is more consistent with electron diffraction data. This function predicts a minimum at the eclipsed form. It appeared that replacing the proton in nitromethane by a chlorine atom the rotation about the C–N is governed by a larger twofold than fourfold term. Theoretical calculations using the 6-311G(d,p) basis set showed that the  $V_2$  term is 2–5 times that of the  $V_4$  term. The stability of the eclipsed form suggests that perhaps the two O $\cdots$ H interactions in the perpendicular form are more unfavorable than the eclipsing N–O and C–Cl bonds (in the perpendicular form), which could be reduced by the larger  $\angle O_4NC$  and  $\angle C1CN$  valence angles.

The presence of the eclipsed form is not surprising if one treats the N–O bond as a delocalized double bond. For example, the anti forms were found to be more stable than the gauche forms in chloroacetyl chloride,<sup>9</sup> bromoacetyl chloride, and bromoacetyl bromide.<sup>10</sup> In chloronitromethane, the eclipsed form is similar to the anti form, and because of the twofold symmetry of the nitro group, the gauche form became the perpendicular form. Our result is not consistent with the conclusion from an earlier ED study where a free rotation about the C–N bond was proposed. A free rotation model was tested by setting  $V_2$  and  $V_4$  of model 4a to zero and an  $R$  factor of 11% was obtained; an agreement poorer than model 4a ( $R = 6.1\%$ ) using a restricted potential (eq 2) with  $V_2 = 0.81(30)$  kcal/mol and  $V_4 = 0.12(40)$  kcal/mol. The infrared spectrum of chloronitromethane in the liquid state was interpreted assuming the presence of only the perpendicular form. Because the dipole moments of the eclipsed and the perpendicular forms are very similar, the liquid state may consist of (1) all eclipsed form or (2) a mixture of eclipsed and perpendicular forms.

The experimental geometrical parameter values compare well with the results from MP2 calculations except for the C–H bond where the experimental error limit is very large. The experimental C–N bond length is 0.010 Å shorter than the MP2 value. All other distances are within 0.003 Å of the calculated MP2 values. The difference between the  $\angle O_4NC$  and  $\angle O_5NC$  valence angles was smaller (4.0°) in the experiment than the theoretical value (7.6°). However, the experimental uncertainties were 1.0°

in each of the valence angles. Comparison with the previous ED study<sup>3</sup> are as follows (new/old):  $r(N-O) = 1.223(1)/1.230(2)$  Å,  $r(N-C) = 1.509(5)/1.493(10)$  Å,  $r(C-Cl) = 1.742(2)/1.765(9)$  Å,  $\angle C1CN = 115.2^\circ(7)/114^\circ(1)$ ,  $\angle CNO_{av} = 117^\circ(1)/116^\circ(1)$ .

The C–Cl bond in chloronitromethane (1.742(2) Å) is significantly shorter than the ones found in chloromethane<sup>11</sup> (1.784(3) Å), chloroethane<sup>12</sup> (1.798(5) Å), and trichloromethane<sup>13</sup> (1.758(2) Å) and close to the C–Cl bond in chlorodifluoromethane<sup>14</sup> (1.747(10) Å). For comparison, the C(sp<sup>2</sup>)–Cl bond in chloroethene<sup>15</sup> is 1.730(4) Å. It appears that introduction of an electron-withdrawing nitro group makes the carbon atom more positive and strengthens the C–Cl bond. Ab initio calculations showed that the C–Cl bond length increases by 0.013 Å when the N–O bond is rotated from eclipsing the C–Cl bond.

The C–N bond length is longer in chloronitromethane (1.509(5) Å) than in nitromethane<sup>16</sup> (1.489(5) Å). The increase in C–N bond could be a result of steric effects of the eclipsed form. The C–N bond for the perpendicular form (0.018 Å shorter) compared well with that for nitromethane. The  $\angle C1CC$  angle in chloroethane is 110.7(3)°, whereas the  $\angle C1CN$  angle in chloronitromethane is 114.8(11)°. The large  $\angle C1CN$  value could also be attributable to the steric environment of the eclipsed form.

Theoretical calculations on the eclipsed and perpendicular forms showed that both the  $r(C-N)$  bond and  $\angle C1CN$  are larger (0.017 Å and 3.9°, respectively) in the more sterically congested eclipsed form than in the perpendicular form. Lengthening the C–N bond and increasing the  $\angle C1CN$  valence angle help to stabilize the eclipsed form because these features decrease the O<sub>4</sub> $\cdots$ Cl steric interaction by increasing the interatomic distance. However, the C–Cl bond is shorter (0.013 Å) in the eclipsed form than in the perpendicular form.

**Acknowledgment.** Q.S. thanks the Petroleum Research Fund for financial support under grant ACS-PRF 38221-B6.

**Supporting Information Available:** Correlation matrix. This material is available free of charge via the Internet at <http://pubs.acs.org>.

## References and Notes

- (1) Tannenbaum, E.; Myers, R. J.; Gwinn, W. D. *J. Chem. Phys.* **1956**, *23*, 42–47.
- (2) Gluzinski, P.; Eckstein, Z. *Spectrochim. Acta* **1968**, *24A*, 1777–84.
- (3) Sadova, N. I.; Volkov, L. V.; Anfimova, T. M. *Zh. Strukt. Khim.* **1972**, *13*, 763–7.
- (4) Hedberg, L. *Abstracts, Fifth Austin Symposium on Gas-Phase Molecular Structure*; Austin, TX, 1974; p 37.
- (5) (a) Hedberg K.; Iwasaki, M. *Acta Crystallogr.* **1964**, *17*, 529. (b) Gundersen, G.; Hedberg, K. *J. Chem. Phys.* **1969**, *51*, 2500.
- (6) Ross, A. W.; Fink, M.; Hilderbrandt, R. L. *International Tables of Crystallography*; Kluwer Academic Publishers: Dordrecht, 1992; Vol. 4, p 245.
- (7) Frisch, M. J.; Trucks, G. W.; Schlegel, H. B.; Scuseria, G. E.; Robb, M. A.; Cheeseman, J. R.; Zakrzewski, V. G.; Montgomery, J. A., Jr.; Stratmann, R. E.; Burant, J. C.; Dapprich, S.; Millam, J. M.; Daniels, A. D.; Kudin, K. N.; Strain, M. C.; Farkas, O.; Tomasi, J.; Barone, V.; Cossi, M.; Cammi, R.; Mennucci, B.; Pomelli, C.; Adamo, C.; Clifford, S.; Ochterski, J.; Petersson, G. A.; Ayala, P. Y.; Cui, Q.; Morokuma, K.; Malick, D. K.; Rabuck, A. D.; Raghavachari, K.; Foresman, J. B.; Cioslowski, J.; Ortiz, J. V.; Stefanov, B. B.; Liu, G.; Liashenko, A.; Piskorz, P.; Komaromi, I.; Gomperts, R.; Martin, R. L.; Fox, D. J.; Keith, T.; Al-Laham, M. A.; Peng, C. Y.; Nanayakkara, A.; Gonzalez, C.; Challacombe, M.; Gill, P. M. W.; Johnson, B. G.; Chen, W.; Wong, M. W.; Andres, J. L.; Head-Gordon, M.; Replogle, E. S.; Pople, J. A. *Gaussian 98*, revision A.9; Gaussian, Inc.: Pittsburgh, PA, 1998.
- (8) Hedberg, L.; Mills, I. M. *J. Mol. Spectrosc.* **1993**, *160*, 117.

- (9) Steinnes, O.; Shen, Q.; Hagen, K. *J. Mol. Struct.* **1980**, *64*, 217.  
(10) Steinnes, O.; Shen, Q.; Hagen, K. *J. Mol. Struct.* **1980**, *66*, 181.  
(11) Bartell, L. S.; Brockway, L. O. *J. Chem. Phys.* **1955**, *23*, 1860.  
(12) Hirota, M.; Iijma, T.; Kimura, M. *Bull. Chem. Soc. Jpn.* **1978**, *51*, 1594.  
(13) Jen, M.; Lide, D. *J. Chem. Phys.* **1962**, *36*, 2525.  
(14) McLay, D. B.; Mann, C. R. *Can. J. Phys.* **1972**, *40*, 61.  
(15) Hui, P. A. G.; Mijlhoff, F. C. *J. Mol. Struct.* **1979**, *54*, 145.  
(16) Cox, A. P.; Waring, S. *J. Chem. Soc., Faraday Trans. 2* **1972**, *68*, 1060.